UNIVERSITY OF CALIFORNIA SAN DIEGO

Dopamine release upon behavior-contingent and non-contingent stimulation of Ventral Pallidum GABA Neurons

A Thesis submitted in partial satisfaction of the requirements
for the degree Master of Science

in

Biology

By

Cody Grayson Sargent

Committee in charge:

Professor Thomas Hnasko, Chair
Professor Byungkook Lim, Co-Chair
Professor Matthew Banghart

2020

The thesis of Cody Grayson Sargent is approved, and it is acceptable in quality and form for publication on microfilm and electronically:

_____

_____

Co-Chair

_____

Chair

University of California San Diego

2020

DEDICATION

To the loving woman that left this world too soon, and to the old man that rambles about swinging a golf club more than I whine neuroscience (haha); I don't want to imagine life without the impact you two have made. Also, to my caring mother that never ceases in being proud, and to the father that at one point lit this fire under my teenage butt – Thank you, and I love you all.

TABLE OF CONTENTS

LIST OF FIGURES

ABSTRACT OF THE THESIS

Dopamine release upon behavior-contingent and non-contingent stimulation of Ventral Pallidum GABA Neurons

by

Cody Grayson Sargent

Master of Science in Biology

University of California San Diego, 2020

Professor Thomas Hnasko, Chair
Professor Byungkook Lim, Co-Chair

The mesolimbic dopaminergic system consists of interconnected brain regions that include the nucleus accumbens (NAc), ventral tegmental area (VTA), ventral pallidum (VP) and lateral habenula (LHb). These circuits have each been implicated in processes that underlie reward and motivation. The VP is a highly heterogeneous structure with varying cell types, projection targets, and functional roles that are only recently being appreciated. Indeed, recent work has revealed a possible opponent role of VP GABA and glutamate neurons in motivated behavior. Specifically, activation of VP GABA neurons, mainly through their projections to the

VTA, induced positive reinforcement; while stimulation of VP glutamate neurons, particularly their projection to the LHb, triggered avoidance. In this work, I further elucidated the mechanism by which VP GABA neurons elicit reward. Particularly, I studied the VP to VTA pathway and assessed the potential for VP GABA terminal stimulation in VTA to trigger dopamine release in the NAc. I showed that stimulation of VP GABA terminals elicits an increase in dopamine release upon both behavior-contingent and non-contingent stimulation. However, both amplitude and duration of dopamine release appeared to be modulated by whether stimulation was contingent on behavior, suggesting a role for motivational or other components in gating the ability of VP GABA inputs to VTA to influence dopamine signaling. These studies provide a foundation for further testing of associated pathways that correlate with reward, learning, and ultimately addiction.

Introduction

The United States alone had an estimated twenty-two million drug addicts in 2013 (NIDA, 2015). This issue coupled with the current annual cost of over $600 billion in treatment demands the exploration of neural mechanism involved and an effective and accessible treatment for drug addiction (Trivedi et al., 2015; NIDA, 2015; NIDA, 2018). The vicious cycle of drug addiction can be defined as the acquisition, maintenance, withdrawal, and relapse to drugs of abuse (Koob et al., 1998; **Figure 1**). An important aspect to consider within this cycle is that acquisition by itself does not trigger relapse since evidence of relapse occurs within individuals that may have been abstinent for decades; such that relapse can be triggered by factors other than drugs of abuse such as associated cues, contexts, and/or stress (Berridge and Robinson, 2016; Robinson and Berridge, 1993; Flagel et al., 2011). A concern with current treatment for drug addiction is the lack of mechanistic understanding of the neurobiology that encodes for reward and related processes that underlie addiction. Addiction is a consequence of drugs of abuse disrupting the homeostatic state within the brain's addiction center, also known as the mesolimbic dopaminergic system (Luscher and Malenka, 2011). Drugs of abuse, such as cocaine, interact with the dopaminergic system of the brain which leads to cascades of long-lasting molecular and synaptic changes associated with drug seeking and relapse behaviors in the dopaminergic system (Russo et al., 2010; Luscher and Malenka, 2011). Therefore, it is critical to fully understand this system, including areas that may have been relatively overlooked, such as the ventral pallidum.

Figure 1. *The cycle of addiction.* Diagram of the cycle of addiction starting at acquisition with the possibility of cycle modifications. (Koob et al., 1998)

The Mesolimbic Dopaminergic System

Current research of addiction pathways within the brain is primarily focused on studying how rewarding stimuli, using optogenetic and pharmacological approaches, interact within the mesolimbic dopaminergic system (Russo et al., 2010; Luscher and Malenka, 2011). The main communicator in the mesolimbic dopaminergic system is the monoamine neurotransmitter known as dopamine (DA) which interacts with its associated receptors. These receptors are the excitatory dopamine receptor-1 (DRD1) and the inhibitory dopamine receptor-2 (DRD2), each located post-synaptically on dopaminergic neurons efferent targets (Binder et al., 2001). The mesolimbic dopaminergic system primarily consists of the ventral tegmental area (VTA) which is located in the midbrain, and the nucleus accumbens (NAc) which is located in the basal forebrain (**Figure 2**). The VTA is dense with dopaminergic neurons, which release dopamine, that project to the NAc among other areas of the brain (Binder et al., 2001). The NAc plays a major role in motivation and reward behavior via the sensitivity to dopaminergic signaling (Binder et al., 2001). Therefore, changes in VTA dopamine neuron activity alter activity in NAc,

and over time contribute to compulsive reward-seeking behaviors and other symptoms that are commonly associated with addiction (Panayi et al., 2005). A few other regions of this system are the lateral habenula (LHb) and ventral pallidum (VP) (**Figure 2**). The LHb is thought to be abundantly glutamatergic and projects to an area caudal to the VTA known as the rostromedial tegmental nucleus (RMTg) which is believed to innervate the VTA via GABAergic projections, and thus leading to inhibition (Yetnikoff et al., 2015). Lastly, the VP plays an unknown level of importance within this system due to the limited understanding within this system, and thus is currently the spotlight for many groups involved in addiction-based neuroscience. (Berridge et al, 2010; Faget et al., 2018).

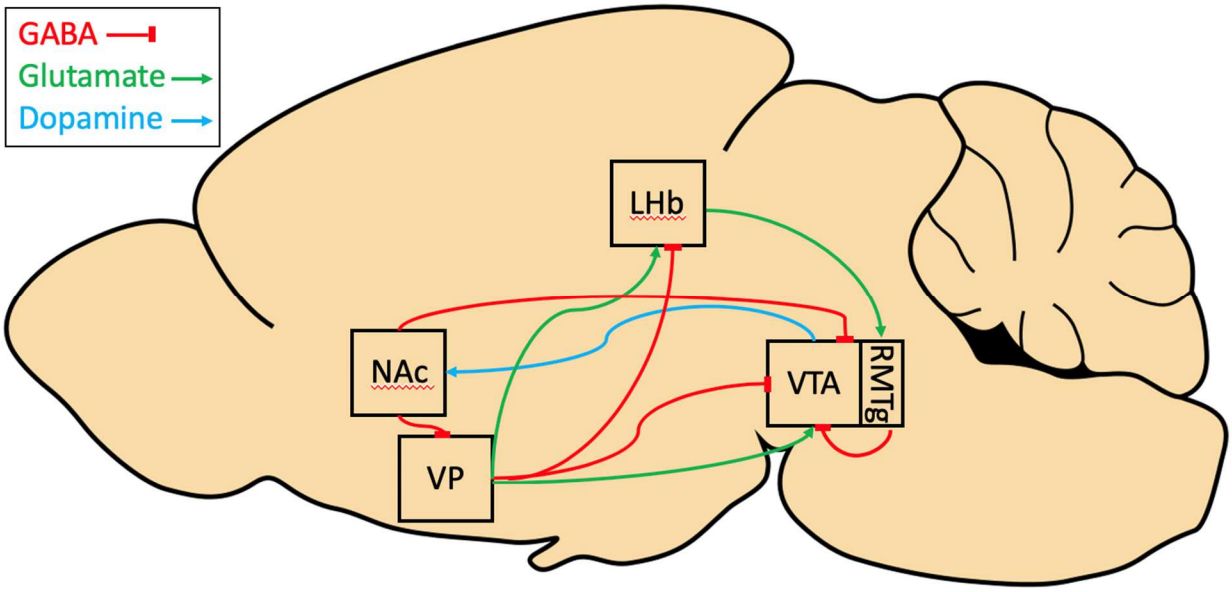

Figure 2. *Neurocircuitry of the mesolimbic dopaminergic system.* Representation of the main areas within the dopamine system and the circuitry of three key neurotransmitters for rewarding and aversive behavior. LHb: lateral habenula, NAc: nucleus accumbens, RMTg: rostromedial tegmental nucleus. VP: ventral pallidum, VTA: ventral tegmental area.

The Ventral Pallidum

The emergence of the Ventral Pallidum (VP) dates back to 1975 when Heimer and Wilson delineated this structure from the substantia innominata (Heimer and Wilson, 1975; Root et al., 2015). Since then, this region has only recently gained attention during discussions pertaining to the neurobiology of mental health, to include addiction (Root et al., 2015). The VP is located at a key anatomical location in the mesolimbic system, integrating information from the NAc and sending dense projections onto the VTA and LHb, three regions playing a critical role in reward and motivation; though the mechanism by which the VP participates into this system is still poorly understood. However, it is know that activation of the VP via electrical stimulation, GABA antagonists, or microinjections of opioids results in reinforcing behavior (Huber and Koob, 1990; Panagis et al., 1995; Stratford et al., 1999; Pecina et al., 2006).

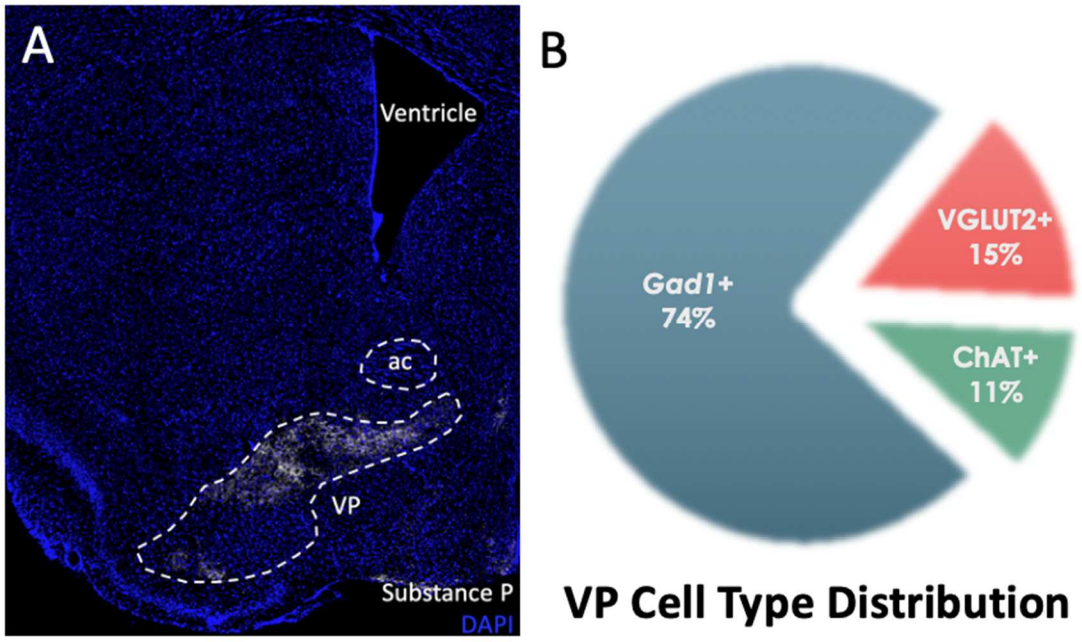

Figure 3. *Morphology and characterization of cell types within the ventral pallidum.* **A)** Representative overview image of the ventral pallidum labeled with substance P immunostaining (white) in a mouse coronal brain section (Bregma: 0.38mm). DAPI in blue. **B)** Distribution of different cell types within the ventral pallidum: 74 percent GABAergic cells (Gad1+), 15 percent glutamatergic cells (VGLUT2+), 11 percent cholinergic cells (ChAT+) (adapted from Faget et al. 2018). ac: anterior commissure, ChAT: choline acetyl transferase, Gad1: glutamic acid decarboxylase 67, VGLUT2: vesicular glutamate transporter 2, VP: ventral pallidum.

Recently, the VP has been determined to be more heterogenous than believed in regard to cell type (Faget et al., 2018; Hur et al., 2005, Root et al., 2015). The VP is mostly comprised of GABAergic cells and additionally is innervated by GABAergic Substance P-expressing fibers, which allow for delineating this structure during characterization (Hjelmstad et al., 2013; Zahm et al., 1996). However, cholinergic neurons and vesicular glutamate transporter-2 (VGLUT2) expressing neurons have also recently been identified (Hur et al., 2005). In recent studies, the anatomical location, relative proportion, and molecular phenotype of each of the three main cell types of the VP have come into sharper focus (Faget et al., 2018). GABAergic neurons, demonstrated in figure 3B, are in fact the most abundant making up 74% of the VP, while glutamatergic and cholinergic cells only make up 15% and 11% of the VP, respectively (Faget et al., 2018; **Figure 3**). Interestingly, while GABAergic and cholinergic neurons were widespread throughout the VP, glutamatergic cells appeared to be mainly concentrated in the ventromedial portion of the VP (Faget et al., 2018).

Past studies have identified subregions of the VP into medial and lateral; and further into ventromedial, dorsal-lateral, caudal, and rostral (Zahm and Heimer 1988; Zahm and Heimer 1990; Zahm et al., 1996). A complete characterization of these subregions will be critical for not only understanding the difference in cell type makeup of each region, but also to best interpret the connectivity to and from the VP. For example, the shell of the NAc projects to the medial portion of the VP while the core of the NAc projects to the lateral portion of the VP (Zahm and Heimer 1988; Zahm and Heimer 1990). Additionally, though the VP is heavily innervated by Substance P-expressing fibers, neurotensin-positive fibers also innervate the ventromedial and dorsolateral portion of the VP (Zahm et al., 1996). At the functional level, the ventromedial and dorsolateral regions also demonstrate different responses to cocaine self-administration. In

regard to rostral versus caudal attributes, Substance P microinjection to the caudal VP elicited a conditioned place preference (CPP) while this effect was absent within the rostral VP (Hasenohrl et al., 1998). Thus, revealing the dense heterogeneity of this structure and the impact it could have on the already complex dopaminergic system.

"Opponent role of VP cell types in motivated behavior"

Multiple studies have shown that activation of the VP elicits reward related behavior (Panagis et al.,1995; Smith and Berridge, 2005). However, these studies did not differentiate by VP cell type. According to the work done by Faget and colleague's, optogenetic activation of VP GABA neurons produced positive reinforcement during a real-time place preference (RTPP) and intra-cranial self-stimulation (ICSS) assay (**Figure 4A & B)**; while their inhibition drove avoidance (Faget et al., 2018). Conversely, an opposite trend was also discovered in regard to glutamatergic neurons (Faget et al., 2018). Indeed, optogenetic activation of VP glutamate neurons induced an avoidance in the place preference assay (**Figure 4C**). However, unlike GABA neurons, inhibition of glutamate neurons did not produce an opposite effect suggesting that these cells might be silent in basal conditions (Faget et al. 2018).

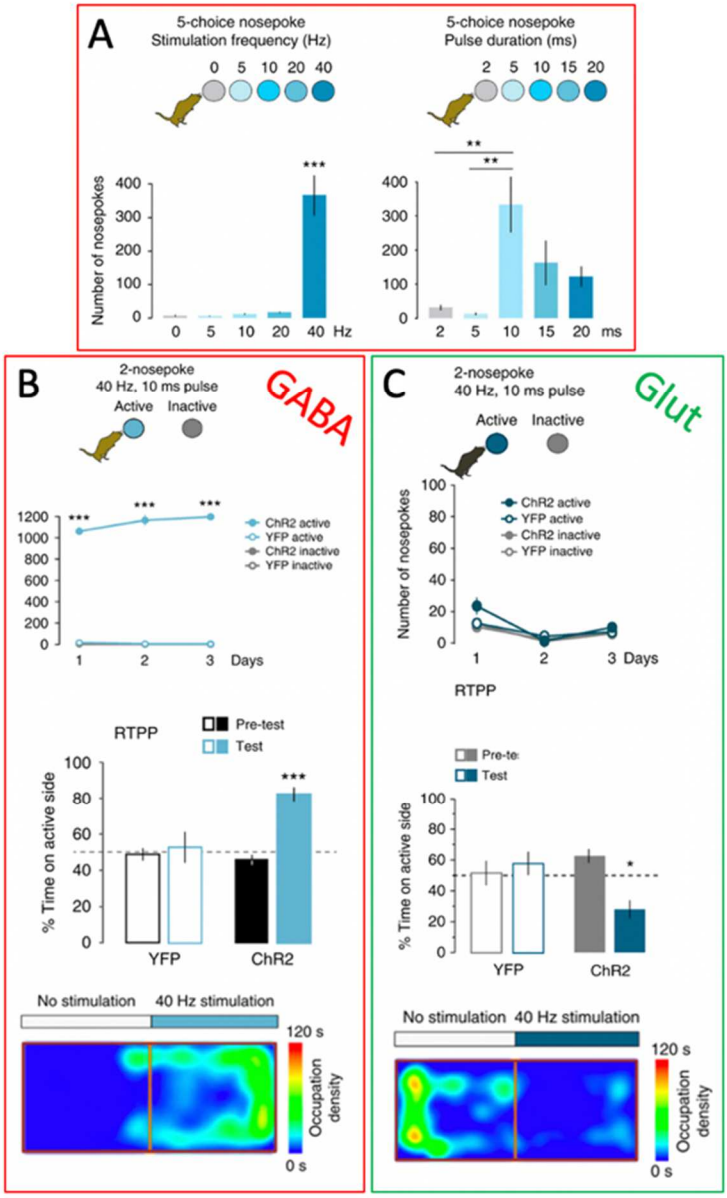

Figure 4. *Stimulation of GABAergic and Glutamatergic neurons supports behavioral reinforcement and aversion, respectively.* **A)** Mice self-stimulate most often when the laser is set to a 40hz frequency at a 10ms pulse duration. **B)** VGAT-Cre mice will self-stimulate and prefer the paired side associated with laser stimulation of GABAergic neurons. **C)** VGLUT2-Cre mice fail to self-stimulate and avoid the paired side associated with laser stimulation of glutamatergic neurons. (Faget et al., 2018)

The rewarding properties of VP GABA neuron stimulation might be counterintuitive in the sense that activation of GABAergic neurons is usually coupled with inhibition of a system and not its excitation (i.e. dopamine neurons in this context). Therefore, the model of

disinhibition must be taken into consideration since it may be able to explain this phenomenon. Such that, VP GABAergic neurons would possibly inhibit VTA local GABAergic interneurons, thus releasing their inhibition onto VTA dopamine neurons and therefore increasing VTA dopaminergic neuron activity. This hypothesis is further supported by Fos data showing an increase in Fos expression in VTA dopamine neurons consequent to VP GABA neurons stimulation (Faget et al. 2018). If this model of disinhibition holds true, then stimulation of VP GABA neurons may indirectly activate dopaminergic neurons within the VTA which then project to the nucleus accumbens to release dopamine and cause reward-related behavior.

Recording In-vivo Dopaminergic Signaling

Behavioral assessment, electrophysiological slice recording, and immunofluorescent tissue histology all agree with the hypothesized theory of VP's opponent control on the mesolimbic dopaminergic system (Stephenson-Jones et al., 2019, Faget et al., 2018, Tooley et al., 2018). However, these studies thus far are deemed incomplete to definitively determine the complete role of the VP. The ability to measure live dopamine signals within the reward hub that is the NAc would help further solve this mechanistic mystery; especially when coupled with optogenetic stimulation and standardized behavioral tasks, which is exactly the idea behind our approach. By injecting a Cre-dependent Channelrhodopsin (light-activated ion channels) virus in genetically modified animals (expressing Cre recombinase in specific cell types, e.g. VGAT-Cre, VGLUT2-Cre), it is possible to activate specific cell types (e.g. GABA or glutamate) in specific brain areas (e.g. VP) via light stimulation using optic fiber brain implant in order to activate the targeted cell type. Also, the recent development of the dopamine biosensor dLight (Patriarchi et

al., 2018) allows to measure changes in dopamine receptor activity within an area of the mouse brain in freely moving mice using fiber photometry (**Figure 5**).

We propose to use each of these tools together in order to test the impact of VP GABAergic terminal stimulation on NAc dopamine release in different behavioral assays. We will measure dopamine transients while the mouse drives the reward (behavior-contingent optogenetic-stimulation of VP GABAergic cells) or passively receives the reward (e.g. non-contingent optogenetic-stimulation of VP GABAergic cells) to assess the overall impact of VP cell type activation on dopamine signaling. These experiments will provide the first evidence of the recruitment of VTA dopamine neurons by VP cell types and will improve our understanding of VP microcircuits in the mesolimbic system. Therefore, we hypothesized that stimulation of GABAergic terminals would recapitulate rewarding behavior while also observing an increase in dopamine signaling within the NAc during behavior-contingent and non-contingent assays.

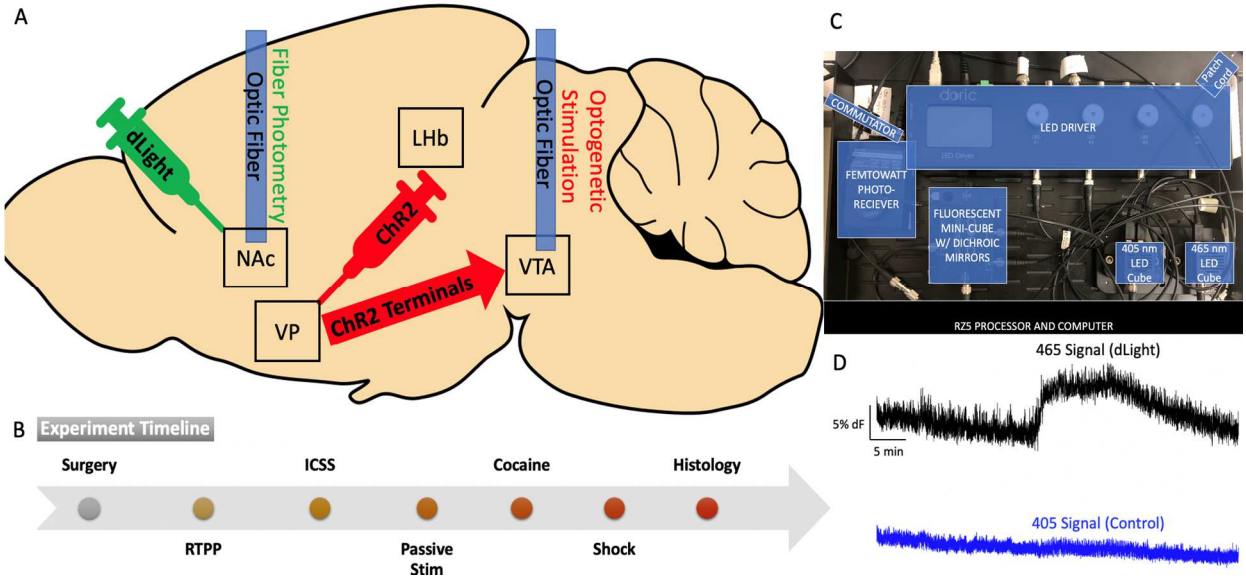

Figure 5. *Experimental approach and fiber photometry setup.* **A)** Diagram of approach for stereotactic surgery. AAV5-CAG-dLight1.1 injected into the NAc with optic fiber placement. AAV1-EF1a-DIO-ChR2:mCherry injected into the VP with optic fiber placed into the VTA. **B)** Experimental timeline. **C)** Labeled DORIC fiber photometry system layout. **D)** Representative transients of fiber photometric signal, 70 minute time window: Black, 465nm dLight signal. Blue, 465nm, control signal.

Materials and Methods

Animals

Homozygous breeders for VGAT-IRES-Cre, knock-in mice were obtained from The Jackson Laboratory: Slc32a1tm2(cre)Lowl. VGAT-Cre mice were C57Bl/6J background. Mice were group housed and maintained on a 12 h light-dark cycle (i.e., light cycle; 7 am–7 pm) with food and water available ad libitum unless noted. Female mice between 6 and 14-weeks old were used and all experiments were conducted during the light phase of the cycle. All protocols were approved by the University of California San Diego Institutional Animal Care and Use Committee.

Stereotactic Surgery

For intracranial injections, mice (>4 weeks) were deeply anesthetized with isoflurane and placed into a stereotaxic apparatus (Kopf). 500 nl of AAV5-CAG-dLight1.1 (8.2×10^{12} genomes/ml, addgene) was infused unilaterally into the left dorsal striatum (LM=-1.6, AP=+1.0, DV=-3.5) or left NAc (LM=-0,8, AP=+1.54, DV=-4.35). 150 nl of AAV1-EF1α-DIO-ChR2:mCherry (2×10^{12} genomes/ml, UNC gene therapy center) was infused unilaterally into the left VP (LM=−1.45, AP=+0.55, DV=−5.35) mm relative to Bregma (Allen Mouse Brain Atlas). Injections were performed at 100 nl/min using Nanoject III (Drummond). The injection tip was left in place for an additional 5 minutes, withdrawn ~0.05 mm, left in place an additional 30 seconds, then slowly retracted. Following viral infusion of AAV1-EF1α-DIO-ChR2:mCherry for optogenetic stimulation, mice were implanted with an optic fiber constructed from 200-µm core multimode optical fiber (FT200EMT, Thorlabs) inserted into a ceramic ferrule (Sparta et al., 2011) in the dorsal striatum (LM=-1.6, AP=+1.0, DV=-3.3) or NAc (LM=-0.8, AP=+1.54, DV=-4.15). or VTA (LM =−0.5, AP =−3.4, DV =−4.0). Following viral infusion of AAV5-CAG-dLight1.1 for recording dLight signal, mice were implanted with an optic fiber constructed from 400-µm core multimode optical fiber (FT200EMT, Thorlabs) inserted into a metallic ferrule in the VTA (LM =−0.5, AP =−3.4, DV =−4.0). Fibers were stabilized in place using dental cement (Lang dental) secured by two skull screws (Plastics One). Animals were treated with analgesic Carprofen (Pfizer, 5 mg/kg s.c.) prior to and the day after surgery. Mice were monitored daily and allowed to recover from surgery >6 weeks prior to subsequent behavioral or physiological assays (All stereotactic surgeries were performed by Lauren Faget)

Fiber Photometry

Mice were implanted with an optical fiber in the dorsal striatum or NAc to deliver blue LED light to excite, and to capture green emission from dLight as a function of dopamine receptor binding. Following a 4-week recovery period, mice were tethered to a computer-controlled dual 465nm and 405nm Doric LED, via a patch cord and optical commutator that allows for free range of motion. Green fluorescence emitted by dLight and autofluorescence (AF; resulting from 405nm light excitation) was captured by a Femtowatt photoreceiver and processed through a TDT RZ5 processor and Synapse Software. During fiber photometric recordings we also used a DPSS 473nm laser to optogenetically excite neurons. We then extracted the data using MATLAB R2019a software. We first applied a controlFit function (Lerner TN et al., 2015) to fit the AF to the dLight signal (computing a least squares polynomial), and calculate the percentage of DF/F ((dLight signal – controlFit AF) / controlFit AF), applying a low pass filter for signals under 10Hz (using the eegfilt function of eeglab package). Data acquired were normalized to a baseline window before the experimental stimulus was delivered, which depended on the assay: RTPP (-2 to -1 sec), ICSS and passively varying durations and frequencies (-1 to 0 sec), passively varying intervals and train stimulations (-0.5 – 0 sec), cocaine injections were normalized only to the 405nm fluorescence, and foot shock (-5 to 0 sec). An area under the curve (AUC) analysis was performed for each assay with varying time windows: RTPP, ICSS, passively varying intervals, and train stimulations was analyzed with a 1 second window; while passively varying stimulation durations and frequencies was dependent on the stimulation time window, cocaine data was a 10 second window, and shock data was 5 second for cue AUC analysis and 0.5 seconds for shock AUC analysis.

Real Time Place Preference

On a baseline (pre-test) day, mice were placed on the border between two adjoining (20 × 20 cm) homogenous gray compartments and the amount of time spent in each compartment was recorded using video tracking software (ANY-maze). Most mice displayed no preference. On the subsequent day, one side was designated active and entry to the active side triggered photostimulation (40 Hz, 10 ms pulse width, 10 mW, 473nm), using the lasers but controlled by an ANY-maze interface (Stoelting). Sessions lasted for 20 min and the amount of time spent in each compartment, distance traveled, speed, and number of crossings were recorded (ANY-maze).

Passive Stimulation

Mice were placed into a clear transfer cage and connected to both patch cords for laser stimulation and fiber photometry recordings for three sessions varying in parameters (controlled by ANY-maze) over two days. On day 1, mice were passively stimulated for a variable amount of time (0.5s, 1s, 2s, and 5s and ranging frequencies (5hz, 10hz, 20hz, and 40hz). On day 2, mice were passively stimulated at varying intervals (2s, 5s, 10s, and 20s) between stimulations. After this the mouse then passively received trains of laser stimulation at 2s, 5s, 10s, and 20s intervals.

Intracranial Self Stimulation

Prior to the first day of testing mice were food-restricted overnight and subsequently provided restricted access of 2g of food overnight per mouse to facilitate behavioral responding. At the beginning of the session, the ferrule was connected to a 50-µm optical patch cord through an optical commutator (Doric Lenses, Canada) and/or fiber photometry cord, and mice were

placed in operant chambers (Med associates) controlled by MedPC IV software. The start of the 45-min session was signaled by a brief tone (2 kHz, 0.5s) and illumination of overhead house light and LED cue lights over the nosepoke holes. The chamber contained two photobeam-equipped nosepoke holes which were each baited at the start of each session with a sucrose pellet (Bio-Serv, F0071). Beam-breaks on the active nosepoke led to: a 0.5s tone, the LED cue lights over the nosepokes turned off for the duration of the timeout period, and the activation of a TTL-controlled DPSS laser (473 nm, Shanghai or OEM laser) set to deliver 10mW (80 × mW/mm2 at 200 μm fiber tip) pulses at 40 Hz (1s) with a 10-ms pulse width controlled by Master-8 (A. M.P.I.) or Arduino stimulus generators. These parameters were changes based on the experimental day, being that after training 1s, 2s, 5s, 10s, and 20s timeout periods were tested on their respective day. Nosepokes that occurred during the timeout period were recorded but without effect. Inactive nosepokes led to identical tone and cue light effects but did not trigger the laser. Laser power was measured using a digital power meter (Thorlabs PM100D/S121C). Mice were tested over 7 days of training and 9 days of fiber photometry recording. Active and inactive nosepokes were switched on a fifth training day to assess for potential side bias.

Intraperitoneal Cocaine Injections

Mice were connected to a patch cord to photometry measurements and placed into a clear transport cage for 70 minutes total while amount of distance traveled, speed, and number of crossings were recorded (ANY-maze). l. The baseline photometry measurement was gathered during the first 10 minutes, and then mice were injected intraperitoneally with 0.9% normal saline and placed back in the cage. After 30 minutes mice were then injected with cocaine

(Sigma) diluted in 0.9% saline chloride to 10mg/kg, 15mg/kg, or 20mg/kg doses. Mice were weighed prior to injection for proper dosing.

Foot Shock

Mice were placed into an operating chamber with a patch cord connected for photometric recordings. Ten electric foot shocks (0.6 mA for 0.5 second) were delivered with variable intervals (randomly chosen from uniform distribution between 45 and 75 seconds) with a predictive cue 5 seconds before shock delivery (3000hz, 90Db). This was performed after all other experiments, since such aversive stimuli can induce sustained fear and anxiety to the context. For analysis, mean fluorescence values were obtained from baseline.

Histology

Mice were deeply anesthetized with a mixture of ketamine (Pfizer, 10 mg/kg i.p.) and xylazine (LLOYD, 2 mg/kg i.p.) and transcardially perfused with 10 ml of phosphate buffered saline (PBS) followed by ~50 ml 4% paraformaldehyde (PFA) at a rate of 5–6 ml/min. Brains were extracted, post-fixed in 4% PFA at 4 °C overnight, and transferred to 30% sucrose in PBS for >48 h at 4 °C. Brains were frozen in isopentane and stored at −80 °C. For virus expression and optic fiber implant site verification, 30-µm coronal cryo-sections were cut using a cryostat (CM3050S, Leica) and collected in PBS containing 0.01% sodium azide. For immunostaining, brain sections were gently rocked 3 × 5 min in PBS, 3 × 5 min in PBS containing 0.2% Triton X-100 (PBS-Tx), and blocked with 4% normal donkey serum (NDS) in PBS-Tx for 1 h at room temperature (RT). Sections were then incubated in one or more primary antibody: chicken anti-GFP, 1:2000, Invitrogen A10262; rabbit anti-DsRed, 1:2000, Clontech 632496; rat anti-

substance P, 1:200, Millipore MAB356, and sheep anti-TH, 1:2000, Pel-Freez P60101-0 in block at 4 °C overnight. Sections were rinsed 3 × 10 min with PBS-Tx and incubated in appropriate secondary antibodies (Jackson ImmunoResearch) conjugated to Alexa488, Alexa594 or Alexa647 fluorescent dyes (5 µg/ml) for 2 h at RT. Sections were washed 3 × 10 min with PBS, mounted on slides, and coverslipped with Fluoromount-G mounting medium (Southern Biotech) ± DAPI (Roche, 0.5 µg/ml).

Imaging

Histochemical characterization were performed on images acquired using a Zeiss AxioObserver Z1 widefield epi-fluorescence microscope (10 × 0.45 NA, 20 × 0.75 NA, or 63 × 1.4 NA objective) and Zen blue software, or on images acquired with NanoZoomer 2 HT (20 × 0.75 NA objective with ×2 lens converter) plus fluorescence module L10387-03 (Hamamatsu). VP boundaries were defined using Substance P staining. Mice were excluded of behavioral studies when mis-placement of the optic fiber was detected.

Statistics

To evaluate statistical significance, data were subjected to two tailed Student's t-tests (RTPP AUC), repeated measure (RM) one or two-way ANOVAs (One-way: RTPP side preference, ICSS AUC, passive stim AUC; Two-way: ICSS nosepokes) followed by Tukey's (RM one-way ANOVA) or Sidak's (RM two-way ANOVA) post hoc analysis, (GraphPad prism v6). Statistical significance was set at $p < 0.05$. All data are presented as means ± SEM unless noted.

Results

We injected AAV-EF1a-DIO-ChR2:mCherry in the VP of four VGAT-Cre mice and implanted an optic fiber on top of the VTA to stimulate VP GABA terminals in the VTA as in Faget et al., 2018. We also injected an AAV virus allowing for expression of the dopamine biosensor DLight1.1 under the control of the ubiquitous promoter CAG, and implanted a second optic fiber on top of the NAc medial shell for measurement of dopamine transients. The first step was to validate functional expression of ChR2 in VP GABA cells and terminals by replicating the behavior observed in Faget et al., 2018, which is a strong preference for the opto-stimulated side in the RTPP assay and strong reinforcing properties in the ICSS assay. A second step was to validate detection of dopamine transients in the NAc medial shell using our fiber photometry system. Finally, upon validation of these two first steps, we aimed at measuring dopamine transients in response to behavior-contingent opto-stimulation of VP GABA terminals in the VTA but also during non-contingent stimulation to evaluate the impact on opto-stim related dopamine transients. One of the four animals was excluded posthoc due to misplacement of the optic fiber which failed to consistently capture dLight activity. Additionally, one of the three remaining mice best demonstrated representative dopamine transients and therefore will be used as an example in the following figures.

Real Time Place Preference

To assess whether or not mice prefer optogenetic stimulation of VP GABA terminals within the VTA we selected to start off with a real time place preference (RTPP) experiment. Indeed, our results demonstrate that mice prefer the optogenetic stimulation paired side 71.03% ± 0.0163) of the time regardless of which side of the apparatus was paired with the laser

stimulation (**Figure 6B**). This validated that the ChR2 injected into the VP should have reached the VTA due to mice showing a strong preference to the side associated with the laser stimulation. Additionally, the amount of line crossings remained constant throughout testing showing an active exploratory behavior of the animals (**Figure 6C**). After four days of testing for real time place preference, animals were tethered with both laser-associated patch cord and fiber photometry patch cord on day 5 to measure dopamine transients during the RTPP assay. We observed an increase in DLight fluorescence (DF/F: (465nm signal – controlfit 405nm signal) / controlfit 405nm signal) at the entry to the paired side – opto-stimulation onset (**Figure 6E**, 1.56% average increase for all mice, $t(2) = 9.664$, $p = 0.0105$) and a decrease in fluorescence at the exit of the paired side - opto-stimulation offset (**Figure 6F**, -1.12% average decrease for all mice, $t(2) = 1.936$, $p =$ ns). This set of data therefore shows that the mice do prefer the laser stimulation of VP GABA terminals in the VTA and that dopamine is released in NAc terminals upon optogenetic stimulation of VP GABA cells.

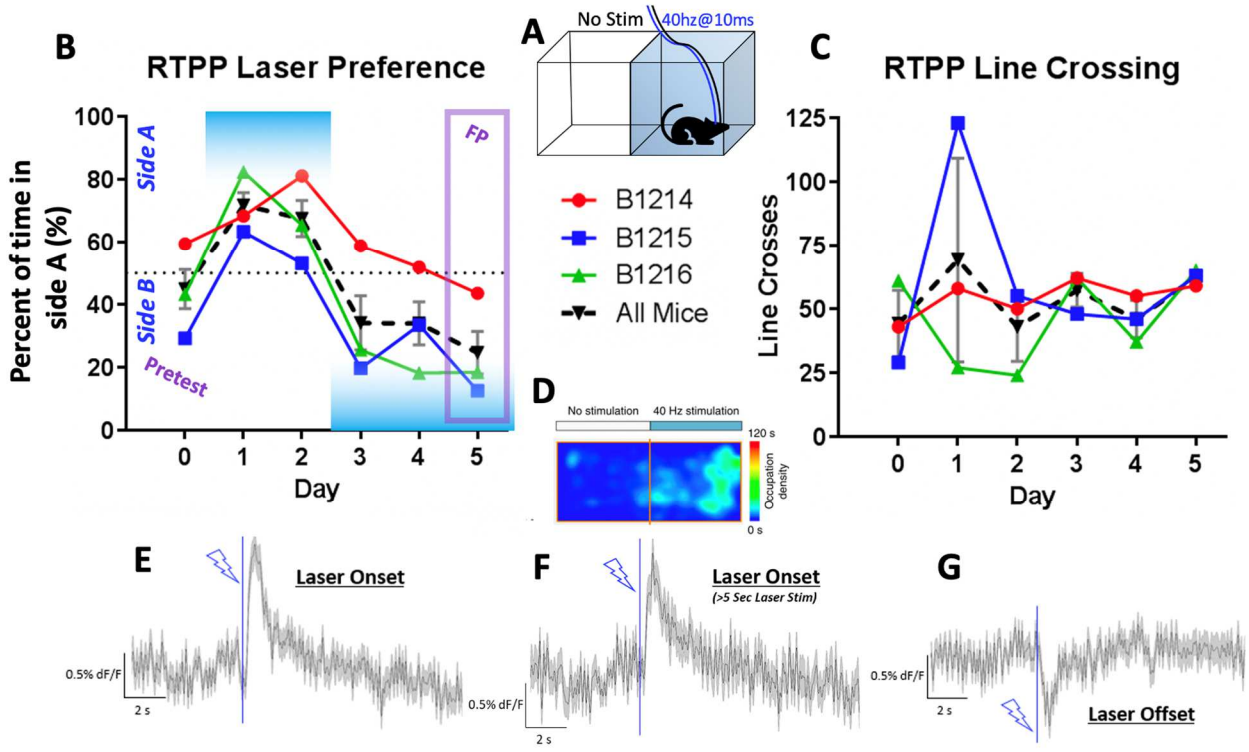

Figure 6. *Increased place preference and dopamine release with place paired optogenetic stimulation of VP GABA neurons.* **A)** Two-chamber box with blue highlighting laser paired side (40hz, 10ms pulse). **B)** Mice demonstrate a preference for the side paired on average 71% of the time. All mice and mean of the mice are shown. **C)** Amount of line crossings per mouse, and the mean (55 ± 5 line crosses) of all mice. **D)** Representative locomotion heat map for mouse B1216 only **E)** Mean dopamine transients across all animals and trials during laser onset triggered from entering the laser paired chamber (1.56% increase, time window: 5s before and 10s after stimulation). **F)** Mean dopamine transients across all animals and trials (only trials where the animal remained in the laser paired side for 5 seconds or greater) during laser onset triggered from entering the laser paired chamber (1.96% increase, time window: 5s before and 10s after stimulation). **G)** Mean dopamine transients across all animals and trials during laser offset triggered from leaving the laser paired chamber (-1.12% decrease, time window: 5s before and 10s after stimulation).

Intracranial Self Stimulation

A 2 nose-poke intracranial self-stimulation (ICSS) was used to determine if mice will learn the task of nose poking into the active laser paired nose poke (1s stim, 40hz, 10ms pulse). This was conducted to determine if the mice not only prefer the stimulation as seen in the RTPP task but also assess whether or not they are motivated to perform a repetitive task to receive this reward. After a few days of training the mice showed a strong preference for the nose poke port

that was paired with the laser while neglecting the nose poke port that was not paired with the laser stimulation (**Figure 7B)**. Indeed, throughout the first week of training mice preferred the active nose poke port (96.5%, 178 active vs. 6 inactive nosepokes per day on average) of the time. Additionally, a second week of training was conducted where we switched the active and inactive nose poke port and mice quickly learned the task and now nose poked (94.9%, 307 active vs. 16 inactive nosepokes per day on average) in the switched active nose poke port. After training, mice were then hooked up to the FP system and dopamine transients were recorded along with incorporating increasing periods of timeout (TO: 1s, 2s, 5s, 10s, and 20s) after laser stimulation where a nose poke in the active port would not illicit a laser stimulation until the timeout was finished. Varying timeout periods were implemented for testing different behaviors, and also for technical reasons (e.g. potential difficulties normalizing after short (1 sec) stimulation) As figure 7c shows, an increase in timeout period accompanied an increase in dopamine transient amplitude response (1s TO: 0.4%, 2s TO: 1.7%, 5s TO: 2.1%, 10s TO: 1.9%, 20s TO: 2.8%) $F_{(1.7,3.5)} = 4.94$, p = ns). This is also shown via the cumulative distribution chart in figure 7D demonstrating that the mice remain motivated to nosepoke as the timeout periods increased in time. Additionally, it shows that the majority of the time the mice learned the new duration of the timeout period due to the mice typically nosepoking immediately after the timeout period expires. Altogether, this data suggests that mice heavily preferred and were well-motivated to work for this burst of stimulation up to a certain period of timeout length.

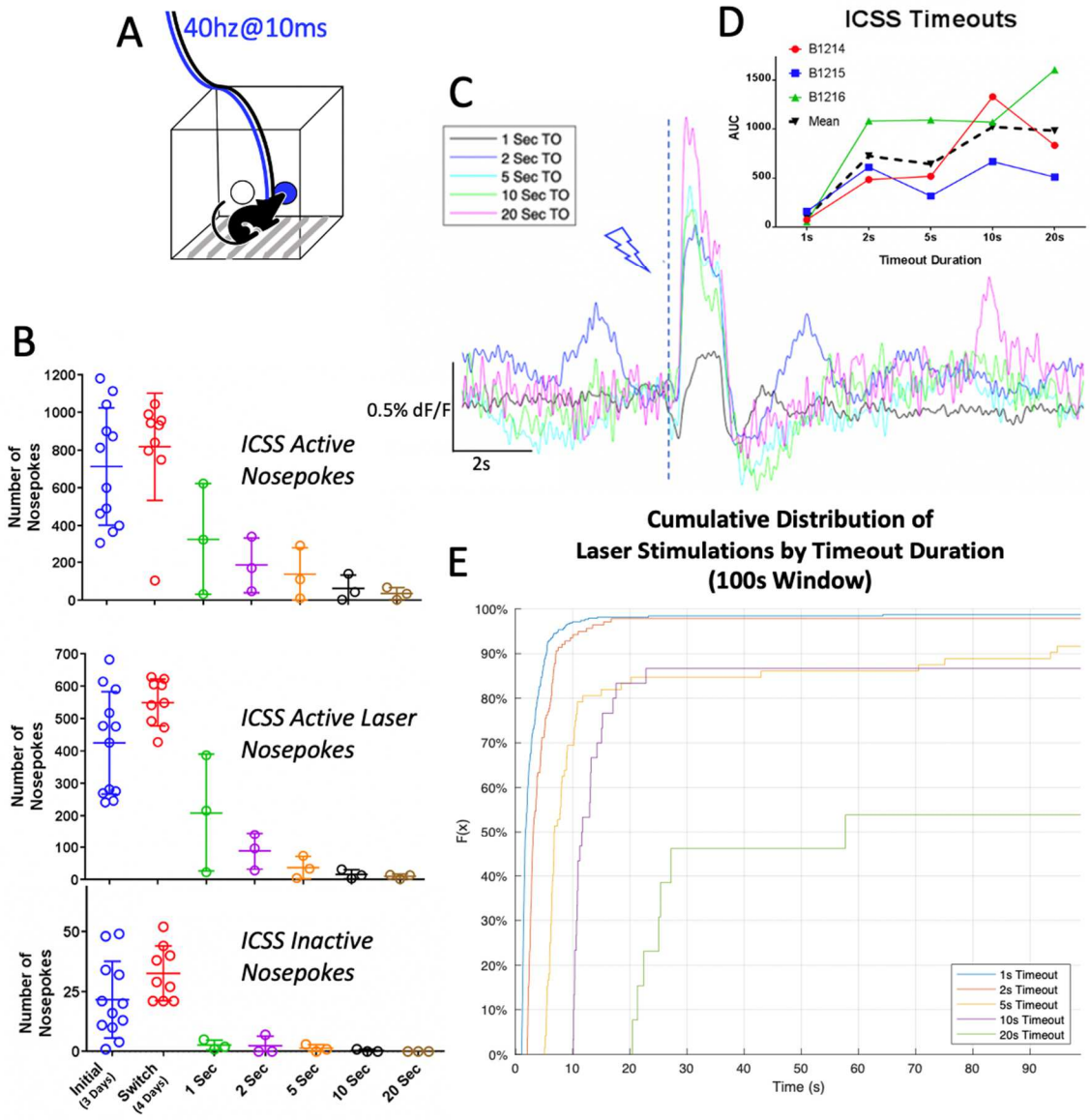

Figure 7. *Longer inter-stimulus interval led to increased dopamine release during contingent self-stimulation of VP GABA neurons.* **A)** Experimental approach of a two-nose poke task with a laser paired nosepoke (40hz @ 10ms pulse). **B)** Amount of nose pokes per increasing timeout interval (Active vs. Inactive, type of nosepoke: $F_{(1,2)} = 49.1$, $p = 0.0198$; Timeout: $F_{(6,12)} = 18.5$, $p = < 0.0001$). **C)** Increase in dopamine transients per increasing timeout (TO) interval. Mouse B1216, average trace: 1s TO: 386 trials, 2s TO: 28 trials, 5s TO: 73 trials, 10s TO: 31 trials, 20s TO: 14 trials. Time window: 5s before and 10s after stimulation. **D)** Dopamine Transients per TO for each animal with mean. (AUC Time window: 1 sec after stimulation) **E)** Cumulative distribution frequency plot (mouse B1216) of laser stimulation, 100s time window.

Passive Stimulation

Here we wanted to assess dopamine transients while the mice passively received optogenetic stimulation to VP GABA terminals in order to compare how behavior-contingent (RTPP and ICSS) assays compared to non-contingent assays. We tested three different parameters: frequency, duration and inter-stimulus interval (ISI). Additionally, for ISI we tested randomized ISI and trains of similar ISI. These experiments suggest that dopamine transients are proportional to the increase in frequency and duration of the stimulation, but do not clearly vary by ISI. As figure 8A shows, the sustained plateau of the dopamine transient is proportional to the stimulus duration, and the increase in dopamine transient amplitude is reflective of the increase in frequency (effect of frequency in the 0.5 second condition: $F_{(1.4,2.7)} = 6.9$, $p = 0.08$,ns; 1 second condition: $F_{(1,2)} = 5.0$, $p =$ ns; 2 second condition: $F_{(1.1,2.2)} = 4.8$, $p =$ ns; 5 second condition: $F_{(1,2)} = 6.4$, $p =$ ns). However, an increase in the interval between stimulations, via interspersed ISI or trains of constant ISI, does not change the amplitude of dopamine transients (Random: $F_{(1,2)} = 0.05$, $p =$ ns; Trains: $F_{(2,4)} = 1.4$, $p =$ ns), which is also consistent with the varying time intervals during the task using trains of stimulations.

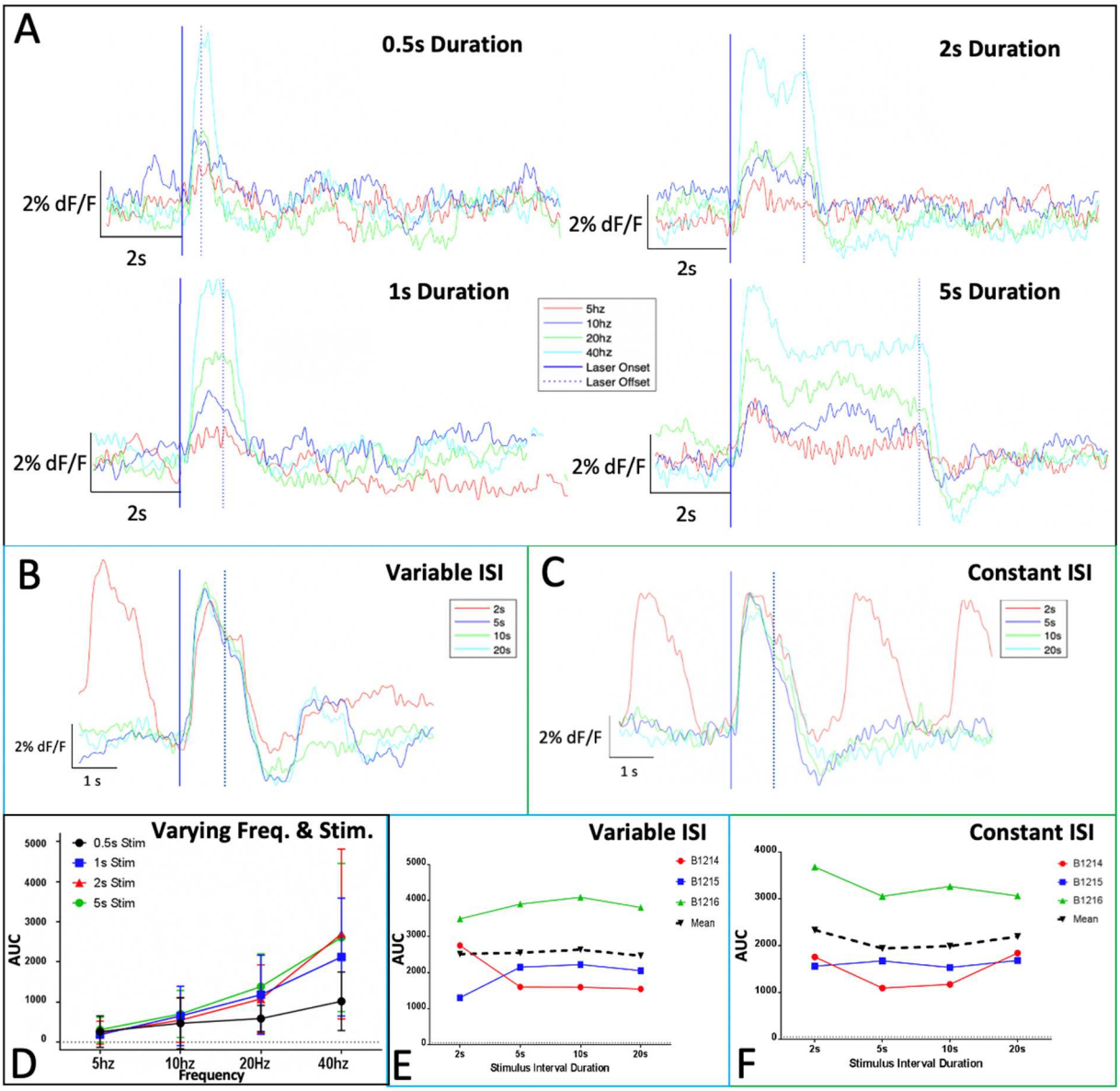

Figure 8. *Non-contingent stimulation of VP GABA neurons led to increased dopamine release proportional to laser frequency and duration, but independent of inter-stimulus interval.* **A)** Increasing the frequency (hertz, hz) and duration of passively delivered stimulations leads to a proportional increase in dopamine transient. Data shown are from Mouse B1216 (Time window: 2s before and 10s after). **B)** Increasing the interval between passive stimulations does not lead to an increase in amplitude of dopamine transients when delivered using a variable ISI or D) constant ISI schedule; Data shown are from Mouse B1216 (time window: 2s before and 5s after). **D, E, F)** Panel A, B, C, respectively, with data included from all three animals. D) AUC time window equals stimulation duration, E) and F) AUC time window equals 1 second.

Intraperitoneal Cocaine Injections

Built into our experimental design were several posthoc validation experiments, such as foot shock and cocaine administration. First, to validate that these transients being measured are also sensitive to non-optogenetic stimulation causing changes in dopamine concentration, we decided to inject cocaine into the mice which causes a large increase in synaptic dopamine levels due to this drug's action to reducing dopamine's synaptic recycling via blocking dopamine active transporters (Huang et al., 2009) Cocaine also causes an increase in locomotor activity, which is directly related to its effect on the dopamine active transporter (Mahler et al., 2014) Indeed, ss shown in figure 9, the levels of dopamine were stable during the control period and saline injections period. However, shortly after an injection of cocaine solution the mouse locomotor activity would typically increase as well as the amount of dopamine release. Of the two mice that elicited a dopamine transient, we observed a 1.9% and 5.1% (Mouse B1215 and B1216, respectively; value extracted from moving mean analysis) increase and plateau over the course of several minutes, and then slowly return to baseline (mouse B1214 was omitted due to patch cord malfunction). These findings were consistent with another cohort of mice which were only injected with dLight with the absence of any optogenetic viral expression.

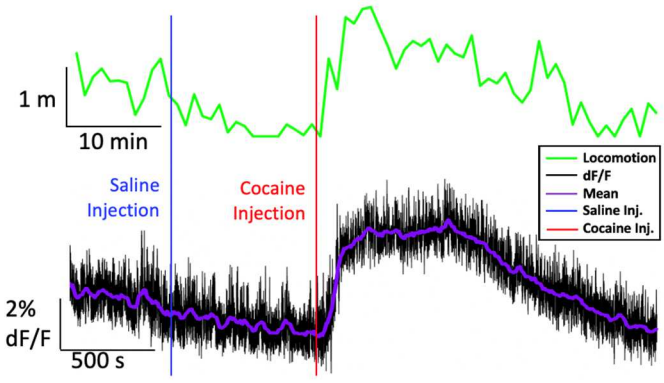

Figure 9. *Intraperitoneal administration of cocaine causes an increase in dopamine release and locomotor activity.* **A)** Increase in locomotion (black) after cocaine injection (red), but not saline injection (blue). **B)** Increase and plateau of dopamine after cocaine injection. Data shown is from mouse B1216 (time window = 70 minutes).

Foot Shock

So far, we have only reported experimental approaches which should drive reward. Here we aimed to analyze the differences in dopamine transients produced from an aversive stimulus such as foot shock. As demonstrated in figure 10 (only mouse B1216), the aversive foot shock induced a small decrease in fluorescence (-1.7%) that lasted the approximate duration of the shock, which was followed by a large rebound increase in fluorescence beginning immediately following the end of the foot shock (3.1%). These data suggested that aversive events modulate dopamine transients in a bidirectional manner.

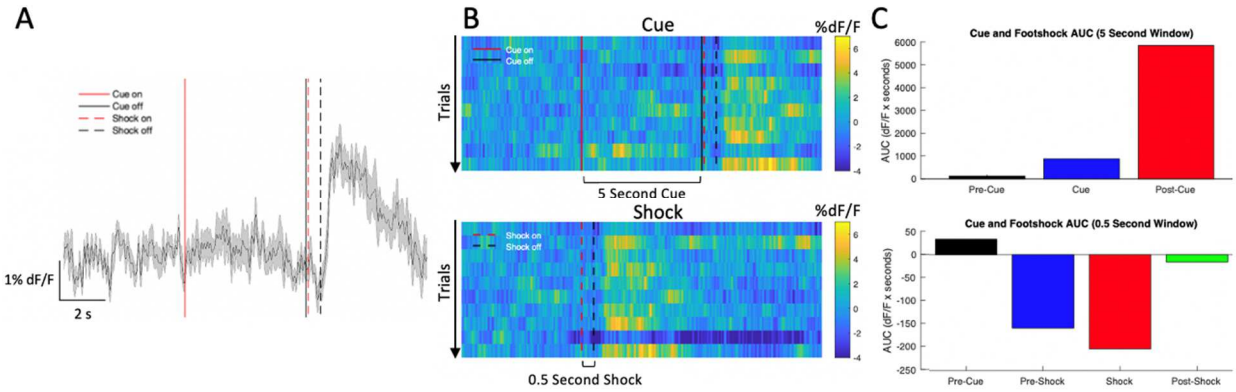

Figure 10. *Aversive foot shock produced a rapid decrease in dopamine followed by a post-shock increase.* **A)** Dopamine transients of ten trials of a 5 second cue (top) followed by a 0.5 second shock (bottom). Time window = 10s before shock and 5s after shock) **B)** Heat maps of the cues and shocks, ten trials. C) Area under the curve (AUC) analysis of 5 second before and after the 5 second cue sound (top), and AUC analysis of 0.5 seconds before the cue, 0.5 seconds before and after the 0.5 second shock stimulus. Data shown is from mouse B1216. AUC time window = 5s (top) or 0.5s (bottom).

Histology

As shown in figure 11, the location of our viral injections and optic fibers are consistent with our targeting. The idea of injecting ChR2 into the VP to infect GABA neurons with the goal of these terminals projecting to the VTA did work. Additionally, the confinement of our dLight viral expression is within the NAc and in close proximity to the implanted optic fiber.

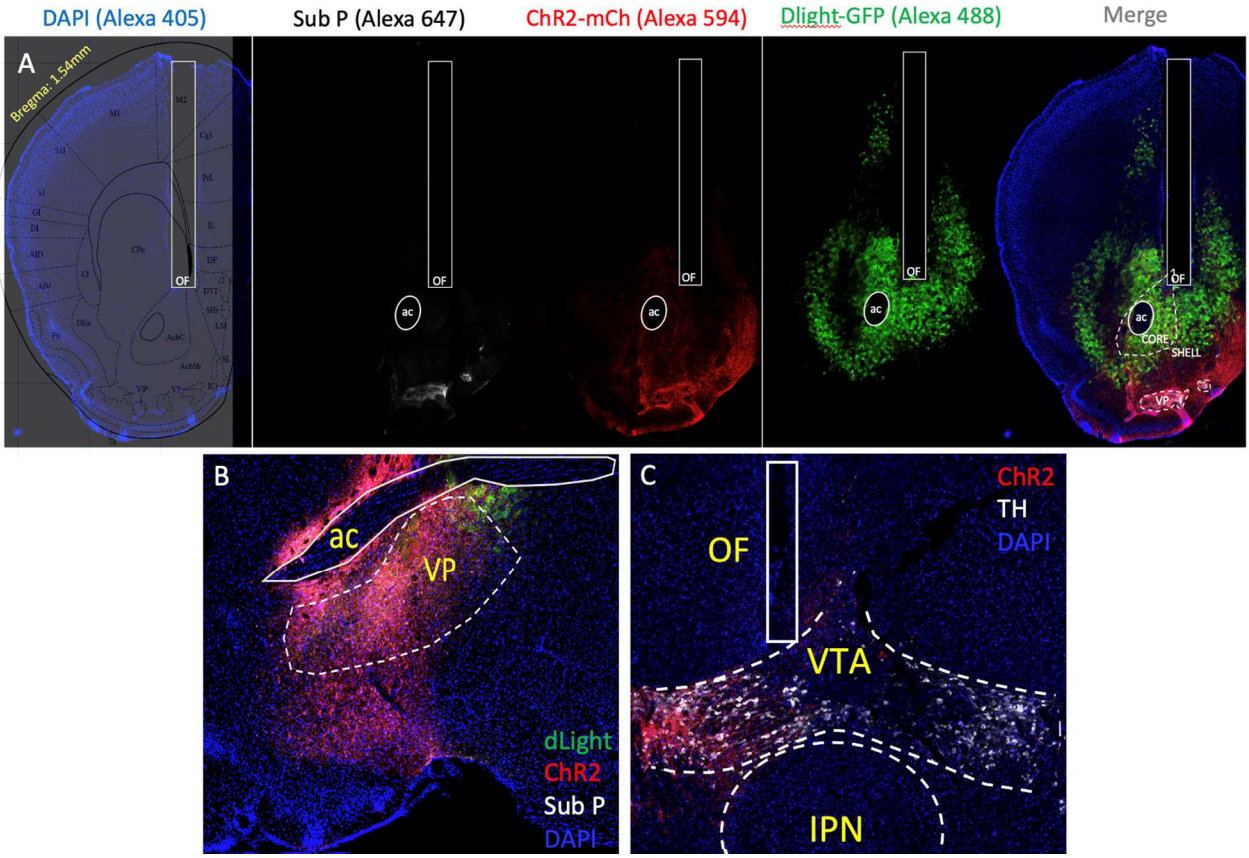

Figure 11. *Histological validation of viral expression and optic fiber placement.* A) Individual channels showing the DLight expression (green) around the NAc along with optic fiber placement, viral expression of ChR2 fibers (red), and the delineation of the VP with substance P (Sub P, white). DAPI in blue. B) ChR2 cell body expression within the VP. C) Delineation of the VTA with tyrosine hydroxylase (TH, white) and evidence of GABAergic ChR2 terminals from the VP along with optic fiber placement. Histology shown is from mouse B1216.

Discussion

Previous studies have shown that neurons within the VP activate in response to reward and reward-related stimuli (Smith and Berridge, 2005; Smith et al., 2009, Tindell et al., 2004) and that electrical stimulation of VP can be reinforcing (Panagis et al., 1995). VP cells are heterogeneous by neurotransmitter content and by projection target. However, recent work demonstrates it is activation of the VP GABA neurons that is reinforcing, particularly projections to VTA (Faget et al., 2018, Stephenson-Jones et al., 2019). We therefore hypothesized that optogenetic stimulation of VP GABA neurons that project to the dopamine neuron rich VTA would lead to an increase in dopamine release within the nucleus accumbens. Consistent with prior reports (Faget et al., 2018, Stephenson-Jones et al., 2019), optogenetic activation of VP GABA terminals in the VTA was sufficient to support behavioral reinforcement, as witnessed during the RTPP and ICSS assays. As predicted, optogenetic stimulation of VP GABA projections during behavioral reinforcement was associated with an increase in dopamine release as demonstrated by increased dLight fluorescence in the NAc, a key VTA projection target. Interestingly, these responses seemed to be larger when the interval between each stimulus (ISI) was longer during when the stimulation was volitional, that is contingent on the animal making a behavioral response. However, this relationship between dopamine release and ISI was only observed during our behavior-contingent assays (RTPP and ICSS) and not during non-contingent passive stimulation; despite the proportional increase in dopamine release we observed when we increased stimulus frequency or duration during passive stimulation. These findings provide new evidence suggesting that GABA release from VP terminals in VTA can promote reward seeking behaviors through an increase dopamine release. And further, we speculate that the impact of VP GABA release on downstream dopamine release is dependent on behavioral contingency.

Stimulation of VP GABA terminals in the VTA elicits an increase in dopamine release in the NAc

The hypothesis that stimulation of VP GABA terminals in the VTA should elicit an increase in dopamine release in the NAc was confirmed. This was concluded via our behavior-contingent assays when coupled with recording dLight fluorescence via fiber photometry. To validate our dLight approach we injected mice with cocaine, which should block the reuptake of dopamine and thus increased dopamine signaling, and successfully recorded a sustained increase in dLight fluorescence, as demonstrated in figure 9 (Huang et al., 2009, Patriarchi et al., 2018). During the behavior-contingent assays, mice were motivated to self-stimulate these VP GABA terminals during ICSS (**figure 7**), and also preferred to remain in the laser-paired chamber during our RTPP assay (**figure 6**); thus, recapitulating the work of Faget and colleagues. As expected, both of these behaviors were coupled with a brief increase in dopamine release in the NAc (Adamantidis et al., 2011; Covey and Cheer, 2019).

The increase in dopamine release in the NAc is presumably due to a disinhibitory mechanism (Bocklisch et al., 2013; Hjelmstad et al., 2013). A similar mechanism has been discovered from the lateral hypothalamus to the VTA, such that GABAergic projections from the lateral hypothalamus to the VTA can mediate appetitive and feeding-related behavior, and vice versa for glutamatergic projections (Nieh et al., 2016). Preliminary data from our lab suggests that both VP GABA and glutamate neurons synapse onto GABA, glutamate, and dopamine neurons in the VTA. Therefore, we proposed that stimulation of VP GABA inhibit VTA GABA neurons, these VTA GABA neurons can no longer inhibit VTA dopamine neurons, and thus an increase in dopamine release in the NAc is observed, thus leading to behavioral reinforcement (Covey and Cheer, 2019).

Dopamine responses vary depending on behavior-contingent or non-contingent context

While both behavior-contingent assays demonstrated dopamine release upon reinforced VP GABA neuron stimulation, our non-contingent assays suggest that behavioral context during this stimulation can alter the dopamine response. To demonstrate this phenomena behind behavioral context, a set of increasing timeout periods were implemented to increase the inter-stimulus interval (ISI) within the ICSS task. Indeed, as timeout periods increased, so did the average peak of dopamine release (**figure 7C**). In contrast, increasing the ISI between non-contingent laser stimulations did not increase the amplitude of dopamine release, despite the proportional increase in dopamine release we observed with increases in stimulus frequency and durations, as demonstrated in figure 8A (Patriarchi et al., 2018).

Another difference between behavior-contingent and non-contingent dopamine responses is the ability to sustain an increase in dopamine release with passively received stimulation, but not during a behavior-contingent context. Such that, passively turning on the laser stimulation for different durations led to an increase in dopamine signal, at least for up to 5s (**figure 8A**). However, during the RTPP assay, even when analyzing just active side visits that lasted at least 5s, the dopamine signal did not persist throughout the duration of optogenetic stimulation and rather it decayed in less than 5s (**figure 6F)**. This peak of dopamine release could be related to the animal initiating the reward or learning that moving into a certain side elicits a reward, compared to the sustained release of dopamine observed during passive stimulation where this volitional engagement and operant type learning is not possible (Stephenson-Jones et al., 2019). In contrast, a decrease in dopamine signal was observed when the animal was exiting the laser paired chamber (**figure 6F**). Since the animal learned that crossing the midline controls the stimulation, it's possible that when exiting we observe a decrease in dopamine that corresponds

to the prediction that there will no longer be a rewarding stimulation (Keiflin and Janak, 2015; Schultz et al., 1997). Otherwise, this decrease could also be explained via a rebound effect such that VP GABA terminals are no longer being stimulated, thus VTA GABA neurons are no longer inhibited, and we witness a rebound firing of VTA GABA above baseline which momentarily over-suppress VTA dopamine neurons.

Experimental Caveats

All four mice demonstrated a strong preference for the optogenetic stimulation, which is supported through our histology by visualizing robust ChR2 expression in VP GABA neurons, along with ChR2 GABA terminals in the VTA around the optic fiber location. However, the delineation of the VP via substance P staining shows that the viral expression was not only restricted to the VP but also (more weakly) found within various regions surrounding the VP, such as the NAc. Therefore, it is possible that a small amount of GABA terminals from surrounding areas, such as the medial shell of the NAc, could have also been stimulated which would result in opposite behaviors (Yang et al., 2018). However, our optogenetic stimulation resulted in reinforcing behavior leading us to believe that the majority of the terminals was associated with VP GABA and not medial NAc terminals.

While the behavioral result consequent to stimulating VP terminals in VTA was consistent, the dLight signals recorded were more variable across the 4 mice. Posthoc analyses offered some explanations. One of our four mice lacked dLight signal from the beginning (B1393), and two of our other mice showing some degree of inconsistent dLight signal throughout testing (B1214 and B1215). Histology confirmed that mouse B1393's optic fiber was

located in the dorsal striatum rather than the NAc and therefore was ruled out from all analysis. However, mouse 1214 and 1215 elicited sufficient dopamine transients throughout testing and analysis to be largely included, with the occasional data set omitted due to lack of signal. Interestingly, there seems to be a slight difference between our mouse with the most consistent signal (B1216) and inconsistent signal; mouse B1216's optic fiber placement was located on top of the NAc medial shell while the other two mice had optic fibers located within the NAc medial shell. Therefore, it's possible to speculate that dLight optic fiber placement would best be implanted right above the medial shell of the NAc rather than any more ventral.

Another important limitation to the ICSS assay was the limited animal mobility due to the two patch cords used for the optogenetic stimulation and FP recordings. Since our setup had two separate commutators this allowed the two cords to wrap around each other. Not only did this apply a lot of torque that could have increased the tension on the head of the mice, but it also could potentially compromise these fragile patch cords, or cause them to slightly become unplugged. For example, when we increased the length of the timeout period the mice appeared to increase their exploration. This may have led to increased rotations and thus twisting of the two patch cords leading to more tension, which therefore caused the mouse to exert additional effort and become hindered to self-stimulate. Therefore, a mixture of this tension and increased periods of timeouts could account for the drastic drop in nosepokes as the timeout period increased. A possible solution could be to use a single commutator system where the two cords can rotate around one another freely, or a complete wireless system.

Going forward

While great leaps have been made to understand the neurocircuitry around reward and addiction, much has yet to be understood or rather spark motivation within the field to assess how other projections to and/or from the VP and associated structures (i.e. VTA and NAc) may have an impact on how reward and addiction may be encoded. The immediate step will be to repeat this scheme of experiments on glutamatergic cre-based mouse lines to examine whether there is a decrease in dopamine release upon stimulation (Tooley et al., 2018), and potentially cholinergic cre-based mouse lines. Additionally, it will be wise to replicate this experiment with improved design, a control group without ChR2, and a greater number of animals to considerably increase the statistical power. Once these VP cell types and their interaction with the NAc via VTA dopamine neurons has been explored, it will be critical to explore regions other than the NAc, such as the lateral habenula, amygdala, and portions of the frontal cortex.

It will be beneficial to look directly at the activity of GABA and dopamine neurons within the VTA via the recording of calcium transients through the utilization of a GCAMP, calcium biosensor, to further validate our microcircuit disinhibitory mechanism hypothesis. These direct approaches though still have limitations due to the restriction of available mouse lines and the need for validation of new viral tools. However, we are working on developing a mouse line that will allow for the cre-dependent GCAMP virus to infect dopamine neurons, along with a flp-dependent ChR2 virus to infect GABAergic neurons (VGAT-flp x DAT-cre mouse line), with ambition to develop the same for glutamatergic lines.

Conclusion

Here we are able to declare with confidence that stimulation of VP GABA terminals within the VTA does cause an increase in dopamine release in the NAc. Providing a plausible explanatory model whereby VP GABA neuron stimulation disinhibits dopamine neurons in the VTA which leads to reinforcing behavior due to increased dopamine release in the NAc.

References

Adamantidis AR, Tsai HC, Boutrel B, Zhang F, Stuber GD, Budygin EA, Tourino C, Bonci A, Deisseroth K, de Lecea L. (2011). Optogenetic interrogation of dopaminergic modulation of the multiple phases of reward-seeking behavior. *Journal of Neuroscience 31*:10829–10835

Allen Institute for Brain Science. (2015). Allen Mouse Brain Atlas. *Allen Mouse Brain Atlas*. Retrieved from hhtp://mouse.brain-map.org

Binder EB, Kinkead B, Owens MJ, Nemeroff CB. 2001. Neurotensin and dopamine interactions. *Pharmacological Reviews 53:*453–486

Berridge KC, Robinson TE. 2016. Liking, Wanting and the Incentive-Sensitization Theory of Addiction. *American Psychologist 71*:670-679

Bocklisch C, Pascoli V, Wong JC, House DR, Yvon C, Roo M, Tan KR, Lüscher C. 2013. Cocaine Disinhibits Dopamine Neurons by Potentiation of GABA Transmission in the Ventral Tegmental Area. *Science 341*:1521-1525

Covey DP, Cheer JF. 2019. Accumbal Dopamine Release Tracks the Expectation of Dopamine Neuron-Mediated Reinforcement. *Cell Reports 27*:481-490

Koob GF, Sanna PP, Bloom FE. 1998. Neuroscience of Addiction. *Neuron 21:467-476*

Faget L, Zell V, Souter E, McPherson A, Ressler R, Gutierrez-Reed N, Yoo JH, Dulcis D, Hnasko TS. 2018. Opponent control of behavioral reinforcement by inhibitory and

Geisler S, Derst C, Veh RW, Zahm, DS. 2007. Glutamatergic afferents of the ventral tegmental area in the rat. *The Journal of Neuroscience 27*: 5730–5743

Hasenohrl RU, Frisch C, Huston JP. 1998. Evidence for anatomical specificity for the reinforcing effects of SP in the nucleus basalis magnocellularis. *Neuroreport 9*:7–10

Heimer L, Wilson, RD. 1975. The subcortical projections of the allocortex: similarities in the neural associations of the hippocampus, the piriform cortex, and the neocortex. *Raven Press; New York*:177-193

Hjelmstad GO, Xia Y, Margolis EB, Fields HL. 2013. Opioid modulation of ventral pallidal afferents to ventral tegmental area neurons. *The Journal of Neuroscience 33*:6454–6459

Howe MW, Tierney PL, Sandberg SG, Phillips PE, Graybiel AM. 2013. Prolonged dopamine signaling in striatum signals proximity and value of distinct rewards. *Nature 500:*575-579

Huang X, Gub HH, Zhana CG. 2009. Mechanism for Cocaine Blocking the Transport of Dopamine: Insights from Molecular Modeling and Dynamics Simulations. *The Journal of Physical Chemistry 113*:2145–2156

Hubner CB, Koob GF. 1990.The ventral pallidum plays a role in mediating cocaine and heroin self-administration in the rat. *Brain Research 508:*20-29

Hur EE, Zaborszky L. 2005. Vglut2 afferents to the medial prefrontal and primary somatosensory cortices: a combined retrograde tracing in situ hybridization study [corrected]. *Journal of Comparative Neurology Comp 483*:351–373

Keiflin R, Janak PH. 2015. Dopamine prediction errors in reward learning and addiction: from theory to neural circuitry. *Neuron 88*:247–263

Lerner TN, Shilyansky C, Davidson TJ, Evans KE, Beier KT, Zalocusky KA, Crow AK, Malenka RC, Luo L, Tomer R, Deisseroth, K. 2015. Intact-Brain Analyses Reveal Distinct Information Carried by SNc Dopamine Subcircuits. *Cell 162*:635–647

Luscher C, Malenka RC. 2011. Drug-evoked synaptic plasticity in addiction: from molecular changes to circuit remodeling. *Neuron 69:*650-663

Stephenson-Jones M, Bravo-Rivera C, Ahrens S, Furlan A, Fernandes-Henriques C, Li B. 2019. Opposing Contributions of GABAergic and Glutamatergic Ventral Pallidal Neurons to Motivational Behaviours. *SSRN Electronic Journal* (bioRxiv) http://dx.doi.org/10.1101/594887

Mahler SV, Vazey EM, Beckley JT, Keistler CR, Mcglinchey EM, Kauflin J, Wilson s, Deisseroth K, Woodward J, Aston-Jones, G. 2014. Designer receptors show role for ventral pallidum input to ventral tegmental area in cocaine seeking. *Nature Neuroscience 17*:577–585

NIDA. 2015. Nationwide Trends. *National Institute of Drug Addiction (NIDA).*

NIDA. 2018. Principles of Drug Addiction Treatment: A Research-Based Guide (Third Addition). *National Institute of Drug Addiction (NIDA)*

Panagis G, Miliaressis , Anagnostakis, Y, Spyraki C. 1995. Ventral pallidum self-stimulation: a moveable electrode mapping study. *Behavioural Brain Research 68*:165–172

Panayi F, Colussi-Mas J, Lambás-Señas L, Renaud B, Scarna H, Bérod A. 2005. Endogenous neurotensin in the ventral tegmental area contributes to amphetamine behavioral sensitization. *Neuropsychopharmacology 30*:871–879

Patriarchi T, Cho JR, Merten K, Howe MW, Marley A, Xiong WH, Folk RW, Broussard GJ, Liang R, Jang MJ, Zhong H, Dombeck D, Zastrow MV, Nimmerjahn A, Gradinaru V,

Williams JT, Tian L. 2018. Ultrafast neuronal imaging of dopamine dynamics with designed genetically encoded sensors. *Science 360*:1-8

Pecina S, Schulkin J, Berridge KC. 2006. Nucleus accumbens corticotropin-releasing factor increases cue-triggered motivation for sucrose reward: paradoxical positive incentive effects in stress? *BMC Biology 4*:8

Robinson TE, Berridge KC. 1993. The neural basis of drug craving: an incentive-sensitization theory of addiction. *Brain Research Reviews 18*:247-291

Root DH, Melendez RI, Zaborszky L, Napier TC. 2015. The ventral pallidum: Subregion-specific functional anatomy and roles in motivated behaviors. *Progress in Neurobiology 130*:29–70

Schultz W, Dayan P, Montague PR. 1997. A neural substrate of prediction and reward. *Science 275*:1593–1599

Smith KS, Berridge KC. 2005. The ventral pallidum and hedonic reward: neurochemical maps of sucrose "liking" and food intake. *The Journal of Neuroscience 25*:8637–8649

Smith KS, Tindell AJ, Aldridge JW, Berridge KC. 2009. Ventral pallidum roles in reward and motivation. *Behavioural Brain Research 196*:155-167

Sparta DR, Stamatakis AM, Phillips JL, Hovelsø N, Van Zessen R, Stuber GD. 2012. Construction of implantable optical fibers for long-term optogenetic manipulation of neural circuits. *Nature Protocols 7*:12–23

Stratford TR, Kelley AE, Simansky KJ. 1999. Blockade of GABAA receptors in the medial ventral pallidum elicits feeding in satiated rats. *Brain Research 825*: 199–203

Tindell AJ, Berridge KC, Aldridge JW. 2004. Ventral Pallidal Representation of Pavlovian Cues and Reward: Population and Rate Codes. *Journal of Neuroscience 24*:1058–1069

Thanos P1, Michaelides M, Piyis YK, Wang GJ, Volkow ND. 2008. Food restriction markedly increases dopamine D2 receptor (D2R) in a rat model of obesity as assessed with in-vivo muPET imaging ([11C] raclopride) and in-vitro ([3H] spiperone) autoradiography. *Synapse 62*:50-61

Tooley J, Marconi L, Alipio JB, Matikainen-Ankney B, Georgio P, Kravitz AV, Creed MC. 2018. Glutamatergic Ventral Pallidal Neurons Modulate Activity of the Habenula–Tegmental Circuitry and Constrain Reward Seeking. *Biological Psychiatry*, *83*:1012–1023

Nieh EH, Vander Weele CM, Matthews GA, Presbrey KN, Wichmann R, Leppla CA, Izadmehr EM, Tye KM. 2016. Inhibitory Input from the Lateral Hypothalamus to the Ventral Tegmental Area Disinhibits Dopamine Neurons and Promotes Behavioral Activation. *Neuron 90*:1286-1298

Yang H, de Jong JW, Tak YE, Peck J, Bateup HS, Lammel S. 2018. Nucleus Accumbens Subnuclei Regulate Motivated Behavior via Direct Inhibition and Disinhibition of VTA Dopamine Subpopulations. *Neuron 97*:434-449.

Yetnikoff L, Cheng AY, Lavezzi HN, Parsley KP, Zahm DS. 2015. Sources of input to the rostromedial tegmental nucleus, ventral tegmental area, and lateral habenula compared: a study in rat. *Journal of Comparative Neurology 53*:2426–2456

Zahm DS, Williams E, Wohltmann C. 1996. Ventral striatopallidothalamic projection: IV. Relative involvements of neurochemically distinct subterritories in the ventral pallidum and adjacent parts of the rostroventral forebrain. *Journal for Comparative Neurology 364*:340-362